

Study on Local Composition of Binary *n*-Alkane for Precise Estimation of Wax Disappearance Temperature

Natee Sa-ngawong and Tawiwat Kangsadan*

Department of Chemical and Process Engineering, The Sirindhorn International Thai-German Graduate School of Engineering (TGGS), King Mongkut's University of Technology North Bangkok, Bangkok, Thailand

Kraipat Cheenkachorn

Department of Chemical Engineering, Faculty of Engineering, King Mongkut's University of Technology North Bangkok, Bangkok, Thailand

Nantiya Inwong and Aungsutorn Mahittikul

Bangchak Corporation Public Company Limited, Bangkok, Thailand

* Corresponding author. E-mail: tawiwat.k@tggs.kmutnb.ac.th DOI: 10.14416/j.asep.2020.02.002

Received: 20 October 2019; Revised: 18 November 2019; Accepted: 25 November 2019; Published online: 19 February 2020

© 2021 King Mongkut's University of Technology North Bangkok. All Rights Reserved.

Abstract

This work aims to investigate the influence of the pure component parameters of *n*-alkanes and assumptions for the solid-phase on the accuracy of wax disappearance temperature (WDT) estimation, using five binary mixtures, consist of *n*-hexane + *n*-hexadecane, *n*-octadecane + *n*-hexadecane, *n*-tridecane + *n*-hexane, *n*-hexadecane + *n*-tetradecane, and *n*-octadecane + *n*-undecane. Perturbed Chain Form of the Statistical Associating Fluid Theory (PC-SAFT) Equation of State (EoS) was implemented to describe solid-liquid equilibrium (SLE) and evaluate its capability for the WDT model. Furthermore, regular solution theory was also applied to SLE description to confirm the prediction from PC-SAFT. The estimated results were compared with the experimental data to examine the accuracy of the provided solution. Reasonable agreement between the predicted and the experimental results was observed. The results were analyzed and theoretical improvement on solutions were suggested.

Keywords: Wax disappearance temperature, Solid-liquid equilibrium, PC-SAFT, Regular solution theory, Binary *n*-alkanes mixtures

1 Introduction

Forming of solid crystal or paraffin (or alkanes) wax in oil is an unwanted phenomenon and potentially harmful to processing equipment, pipeline, or even in the motorized engine, and this can end up in obviously redundant expenses [1]–[4]. Different environment, pressure, temperature, or composition may yield drastically change in behavior of precipitation [2], [3], [5]. Therefore, the development of precise evaluation

by techniques and estimated tools for the determination of this wax behavior is very crucial.

Two common parameters including wax appearance temperature (WAT) and wax disappearance temperature (WDT) are used to partially identify the oil utilization limit. These two parameters describe the same phenomena, but with different point of view. The WAT, known as cloud point, is a temperature of the first crystal appearance by cooling process. WAT is an important parameter, especially in the oil industry

which used to identify the point at which oil can be fully utilized. The WDT is a temperature at which the last crystal re-dissolves in oil by heating process [3], [6]. Experiment studies show that the WAT and the WDT are not necessary to be at the same equilibrium point, where their values depend on the measurement technique [3], [6]. However, previous studies showed that WDT represented a true solid-liquid equilibrium (SLE), while WAT did not [3], [6]. Additionally, the difference between WAT and WDT can be very significantly large.

Ronningsen *et al.* [7], used microscopy to measure the WAT and the WDT of a North Sea crude oil. It was shown that the WDT is 0–28°C higher than the WAT. Dunn [8] applied Differential Scanning Calorimetry (DSC) for heating and cooling scans to determine the melting point and the freezing point of a pure fatty acid methyl esters of methyl palmitate, methyl stearate, and methyl oleate, and found that the melting point is 3–20°C higher than the freezing point.

Since the formation of wax leads to several problems in cold environment, it is essential to understand a formation behavior. Many researchers developed a reliable measurement of the WAT and the WDT, and thermodynamic models to correctly predict. Mirante *et al.* [1], used modified UNIFAC for the liquid-phase and different solid-phase models to estimate the WAT of different solutions. Similar work was conducted by Parsa *et al.* [3], they estimated the WDT using a different liquid-phase model and solid-phase model, and compared with their experimental data.

For an industrial application, it is indeed to correctly estimate the WAT and the WDT in multicomponent systems. However, such calculation requires a massive number of parameters. Additionally, key parameters are unknown. It is interesting that these key parameters can be used as database for the prediction of the WAT and the WDT. Therefore, finding key thermodynamic-parameters are significantly important.

In this present work, mathematical perspective using thermodynamic expression may lead to an undeniable complex behavior of the wax. To evaluate the influence of thermodynamic parameters, therefore, the simple case of binary mixtures of *n*-paraffins including *n*-hexane + *n*-hexadecane [$C_6 + C_{16}$], *n*-octadecane + *n*-hexadecane [$C_{18} + C_{16}$], *n*-tridecane + *n*-hexane [$C_{13} + C_6$], *n*-hexadecane + *n*-tetradecane [$C_{16} + C_{14}$], and *n*-octadecane + *n*-undecane [$C_{18} + C_{11}$]

were studied.

In order to properly evaluate the estimated WDT, the applied solution has to be appropriately selected based on the capability of the solution. For systematic studies in this work, the appropriate solution that closes to the fundamental theory has to be carefully chosen.

Up to now, the major issue in the thermodynamic description shows no exact solutions that can be claimed for real situations, in which the precision of solution may not totally represent the real behavior. For the industrial application, this work applied the Equation of State (EoS) as the Perturbed Chain form of the Statistical Associating Fluid Theory (PC-SAFT) to describe the behavior of the WDT. Similar to the fundamental EoS and unlike the other solutions, PC-SAFT makes use of statistical mechanical methods, particularly the perturbation theory of Barker and Henderson to represent hard-chain as a reference fluid, which is proved to be physically base and robust for representing complex fluid [2]. Additionally, a unique benefit of using PC-SAFT is that, each term in the equation refer to the different type of the molecular interaction in which it may give a close representation due to the nature of the system. For instance, the basic interactions that must be included are the hard-chain reference contribution (A^{hc}/NkT) and the dispersion contribution (A^{disp}/NkT) with possible additional interaction of the association (A^{assoc}/NkT), the polar interaction (A^{dipol}/NkT), and the electrostatic interaction (A^{elec}/NkT) [2], [9]–[12].

Moreover, this work also implemented the regular solution theory to verify the estimated WDT from PC-SAFT. In the end, the estimated results were compared with the experimental WDT of the reference, analyzed the parameter influence, and suggested the improvement of the solution.

2 Thermodynamics Model

2.1 Solid-liquid equilibrium

Theoretically, the description for the SLE is taken from the equilibrium at the triple point temperature. As described by Prausnitz *et al.* [13], there is not significant difference between triple point and normal melting point, in terms of both temperature and enthalpies of fusion, for most substances. Therefore, practically, it is acceptable to replace both temperature and enthalpies of fusion at the triple-point temperature by normal melting temperature.

Thus, fugacities for component i in all phases must be equal at equilibrium as defined in Equation (1).

$$f_i^L = f_i^S = f_i^V \quad (1)$$

where f_i^L , f_i^S , and f_i^V are the fugacity of component i in liquid-phase, solid-phase and vapor-phase, respectively. Fugacities corresponding to each liquid-phase and solid-phase are expressed by [3], [13]:

$$f_i^L = x_i^L \gamma_i^L f_{pure,i}^L \int_{P_0}^P \frac{v_i^L}{RT} dP \quad (2)$$

$$f_i^S = x_i^S \gamma_i^S f_{pure,i}^S \int_{P_0}^P \frac{v_i^S}{RT} dP \quad (3)$$

where $f_{pure,i}^L$ and $f_{pure,i}^S$ are the fugacity of pure component i in liquid-phase and solid-phase, respectively. x_i is the mole fraction of component i , γ_i is the activity coefficient of component i , and v_i is the molar volume of component i . R is the gas constant, T is temperature, and P is pressure. In a case where the pressure influence is insignificant, the integral term of pressure in Equations (2) and (3) can be omitted. To identify which temperature is the WDT, the relation between the fugacity and SLE is used as expressed in Equation (4):

$$\ln \left(\frac{f_{pure,i}^L}{f_{pure,i}^S} \right) = \frac{\Delta H_i^{fus}}{RT} \left(1 - \frac{T}{T_{fus,i}} \right) + \frac{1}{RT} \int_{T_{fus,i}}^T \Delta C p_i dT - \frac{1}{R} \int_{T_{fus,i}}^T \frac{\Delta C p_i}{T} dT \quad (4)$$

where ΔH_i^{fus} is the fusion enthalpy at the fusion temperature $T_{fus,i}$, and $\Delta C p_i$ is the difference between heat capacities of component i in liquid-phase and solid-phase ($\Delta C p_i = C p_i^L - C p_i^S$). It should be noted here; the fusion enthalpy and the fusion temperature in this work is referred to the crystalline I – liquid transition only. However, in the case that the component has the phase contribution of the other crystalline formations, for instance, crystalline II-I, and crystalline III-II, then Equation (4) can be revised in the form of Equation (5):

$$\ln \left(\frac{f_{pure,i}^L}{f_{pure,i}^S} \right) = \frac{\Delta H_i^{fus}}{RT} \left(1 - \frac{T}{T_{fus,i}} \right) + \frac{1}{RT} \int_{T_{fus,i}}^T \Delta C p_i dT - \frac{1}{R} \int_{T_{fus,i}}^T \frac{\Delta C p_i}{T} dT + \frac{\Delta H_i^{tr}}{RT} \left(1 - \frac{T}{T_{tr,i}} \right) \quad (5)$$

where ΔH_i^{tr} is the transition enthalpy at the transition temperature $T_{tr,i}$ of the interested crystalline transformation. However, in this work, ΔH_i^{tr} and $T_{tr,i}$ are considered only the crystalline II-I transformation, since this is sufficient to observe the influence of the crystalline transition to the estimated result. In the case that the other crystalline transformations are expected, it requires the improvement of Equation (5).

According to Meighani *et al.* [2], Equation (5) can be classified into two main categories based on the following assumptions for the miscibility of solid-phase:

Category 1: The hydrocarbon in the solid-phase is usually formed as a solid solution. Then, Equation (5) can be separated into two parts according to the fugacity as, f_i^L and f_i^S . For f_i^L or the fugacity of component i in liquid-phase, it is usually estimated from vapor-liquid equilibrium (VLE) relation as Cubic EoS or Soave-Redlich-Kwong EoS. This f_i^L can also be either estimated by any available activity coefficient models. While f_i^S or the fugacity of component i in solid-phase is estimated from SLE relation, which is usually done by the activity coefficient model in the excess Gibbs free energy form (or excess Gibbs free energy model) such as Wilson, NRTL, and UNIQUAC [1].

Category 2: Based on the multiple solid-phase model, each precipitated component is considered as an immiscible separated solid-phase, which is immiscible to each other [2], [13], [14]. While the liquid-phase is estimated from VLE relation, as previously mentioned in categories 1). Then, Equation (5) can be modified according to this assumption, as expressed in Equation (6):

For the complex solid-phase, the two assumptions mentioned above are no longer valid because the f_i^S cannot be improved as described by Tumakaka *et al.* [12]. However, this can be achieved by treating the system as a pseudo chemical reaction and estimating the phase change temperature or WDT by equilibrium constant.

$$\ln\left(\frac{1}{x_i^L \gamma_i^L}\right) = \frac{\Delta H_i^{fus}}{RT} \left(1 - \frac{T}{T_{fus,i}}\right) + \frac{1}{RT} \int_{T_{fus,i}}^T \Delta C p_i dT - \frac{1}{R} \int_{T_{fus,i}}^T \frac{\Delta C p_i}{T} dT + \frac{\Delta H_i^{tr}}{RT} \left(1 - \frac{T}{T_{tr,i}}\right) \quad (6)$$

Therefore, this work used the multiple solid-phase equation, which was simpler to analyze the influence of SLE parameters ΔH_i^{fus} , ΔH_i^{tr} , and $\Delta C p_i$. Moreover, this form of equation could describe the influence of the solid-phase formations to the accuracy of the prediction, as well as, the solid formation trend of the substance.

2.2 PC-SAFT equation of state

This study adapted the original PC-SAFT EoS with the non-associating term developed by Gross *et al.* [15] to estimate the activity coefficient in the liquid-phase. This equation is used to describe the VLE relation with the residual Helmholtz free energy as given by Equation (7):

$$\frac{A^{res}}{NkT} = \frac{A^{hc}}{NkT} + \frac{A^{disp}}{NkT} \quad (7)$$

For the non-associating system, the equation requires three specific pure component parameters, m is the compound's segment number, σ is the temperature-independent segment diameter, and ε/k is the segment dispersion energy parameter which describes the dispersive interaction [15]. The relationship between the activity coefficient γ_i and the fugacity coefficient φ_i provided by PC-SAFT can be obtained as follows [Equation (8)]:

$$\ln \varphi_k = \frac{\mu_k^{res}(T, v)}{kT} - \ln Z \quad (8)$$

where the chemical potential μ_k^{res} and the compressibility factor Z are defined in Equations (9) and (10), respectively.

$$\begin{aligned} \frac{\mu_k^{res}(T, v)}{kT} - \ln Z &= \frac{A^{res}}{NkT} + (Z-1) + \left(\partial \frac{A^{res}}{NkT} / \partial x_k \right)_{T, v, x_{i \neq k}} \\ &- \sum_j \left[x_j \left(\partial \frac{A^{res}}{NkT} / \partial x_j \right)_{T, v, x_{i \neq j}} \right] \end{aligned} \quad (9)$$

$$Z = 1 + \eta \left(\partial \frac{A^{res}}{NkT} / \partial \eta \right) \quad (10)$$

Then, the correlation between the activity coefficient and the fugacity coefficient are described as follows:

$$\begin{aligned} \gamma_i(T, P, \{x_i\}, f_i^o) &= \frac{\varphi_i(T, P, \{x_i\})P}{f_i^o(T, P_i^o)} \\ &= \frac{\varphi_i(T, P, \{x_i\})P}{\varphi_i^o(T, P)P_i^o} \end{aligned} \quad (11)$$

where the standard-state pressure P_i^o equals to the mixture pressure P in this work, therefore, Equation (11) becomes [Equation (12) or (13)]:

$$\gamma_i(T, P, \{x_i\}, f_i^o) = \frac{\varphi_i(T, P, \{x_i\})}{\varphi_i^o(T, P)} \quad (12)$$

or

$$\gamma_i(T, P, \{x_i\}, f_{pure,i}^o) = \frac{\varphi_i(T, P, \{x_i\})}{\varphi_{pure,i}(T, P)} \quad (13)$$

2.3 Regular solution theory

Besides the PC-SAFT, this work also used the regular solution theory for the comparison. The regular solution theory describes the activity coefficient as a function of molar volume and solubility corresponding to each phase as given in Equations (14) and (15) [2], [3], [16]:

$$\ln \gamma_i^L = \frac{v_i^L (\bar{\delta}^L - \delta_i^L)^2}{RT} \quad (14)$$

$$\ln \gamma_i^S = \frac{v_i^S (\bar{\delta}^S - \delta_i^S)^2}{RT} \quad (15)$$

where δ_i^L and δ_i^S are the solubility parameters of component i corresponding to liquid-phase and solid-phase, respectively. $\bar{\delta}^L$ and $\bar{\delta}^S$ are mean solubility parameters of liquid-phase and solid-phase as expressed in Equations (16) and (17), respectively:

$$\bar{\delta}^L = \sum_i \phi_i^L \delta_i^L \quad (16)$$

$$\bar{\delta}^S = \sum_i \phi_i^S \delta_i^S \quad (17)$$

where ϕ_i^L and ϕ_i^S are the volume fractions of component i in liquid-phase and solid-phase as expressed in Equations (18) and (19), respectively:

$$\phi_i^L = \frac{x_i^L v_i^L}{\sum_i x_i^L v_i^L} \quad (18)$$

$$\phi_i^S = \frac{x_i^S v_i^S}{\sum_i x_i^S v_i^S} \quad (19)$$

The solubility parameter of component i in liquid-phase are available in any database. However, the group contribution Hansen partial solubility parameter was selected in this work [17]. This method has potentially described the solubility parameter, especially for isomer compounds using second order group contribution. The Hansen partial solubility parameter describes the total solubility parameter as a separate function of dispersion (δ_d), polar (δ_p), and hydrogen-bonding (δ_{hb}) [17].

However, the solubility of component i in solid-phase is described as [Equation (20)]:

$$\delta_i^S = \left(\frac{\Delta H_i^{fus}}{v_i} + (\delta_i^L)^2 \right)^{0.5} \quad (20)$$

where the molar volume (in $\text{cm}^3 \cdot \text{mol}^{-1}$) at equilibrium for this regular solution theory is expressed by [Equation (21)]

$$v_i^L = v_i^S = v_i = \frac{MW_i}{D_{i,25}^L} \quad (21)$$

where $D_{i,25}^L$ is the liquid-phase density (in $\text{g} \cdot \text{cm}^{-3}$) of component i at 25°C and calculated from the following

empirical correlation [4]:

$$D_{i,25}^L = 0.8155 + (0.6272 \times 10^{-4}) MW_i - \frac{13.06}{MW_i} \quad (22)$$

3 Methodology and Materials

3.1 Methodology

From the industrial point of view, the deviation in the estimation of temperature that less than 1 K at specific iteration is not significant. The acceptance is also applied for a density, which is an input parameter for PC-SAFT. Consequently, the accuracy of the estimation in this work has to limit by an acceptable threshold. The resolution for a temperature is decreased or increased by 1 K at any given iteration. For the acceptable value of the WDT, the difference between terms in Equations (4)–(6) on the left hand side and the right hand side of the equal sign must be less than ± 0.05 . Each iteration of the estimated density results in the deviation between the estimated pressure (or the fluid pressure) and the given pressure of the system. At this point, the deviation between the two pressures must be less than $\pm 1\%$. With this approach, the estimation can be achieved with an acceptable error. Furthermore, this work focused on the influence of thermodynamic parameters on the trend of the estimated WDT, therefore, it did not require to achieve a very fine resolution. Then, the accuracy of the estimation is determined by the root-mean-square deviation (RMSD) of temperatures as defined by following Equation (23):

$$RMSD = \sqrt{\frac{\sum_{i=1}^n (T_i^{\text{exp}} - T_i^{\text{cal}})^2}{n}} \quad (23)$$

where T_i^{exp} and T_i^{cal} are the experimental WDT and the estimated WDT according to Equations (4)–(6), respectively, and n is the number of experimental data points excluding from the fixed point data.

3.2 Material

It is essential that the experimental database or even correlation must be extremely accurate to determine the exact pure component parameter and to avoid the error accumulation by each parameter, which results to the

over or under estimation, leading to false evaluation. Therefore, in this work, the pure component parameter, especially phase-change properties (ΔH_i^{fus} , ΔH_i^{tr} , $T_{fus,i}$, $T_{tr,i}$, ΔCp_i) according to the WDT are depended on the reliable source.

Nevertheless, some literatures have usually omitted the heat capacity ΔCp_i because its contribution to the prediction result is very small [1], [13], [18] and it is difficult to experimentally measure and to obtain the suitable correlation to estimate ΔCp_i at melting temperature (T_{fus}) in the stable phase [19], [20]. By neglecting this parameter can yield drastically difference, especially in the multicomponent system. Moreover, the heat capacity is extremely influenced with the mixture containing higher molecular weight of *n*-alkane more than the lighter one [21]. Therefore, the degree of influence from the heat capacity was investigated in this work with the assumption that the heat capacity ΔCp_i was constant, independent of temperature T . These ΔCp_i parameters are represented in Table 1.

4 Results and Discussion

Pure component parameters and estimated wax disappearance temperatures for five different mixtures are presented in Table 1 and Table 2, and Figure 1–6, respectively.

Table 1: Pure-component parameter for SLE equation

Compound	$T_{fus,i}$ [K]	ΔH_i^{fus} [kJ mol ⁻¹]	ΔCp_i^a [J mol ⁻¹ K ⁻¹]	$T_{tr,i}$ [K]	ΔH_i^{tr} [kJ mol ⁻¹]	Ref.
<i>n</i> -hexane	177.97	12.87	46.87	-	-	[22]–[26]
<i>n</i> -undecane	247.40	22.25	-49.24	236.35	6.60	[25], [27]
<i>n</i> -tridecane	267.79	28.50	-111.45	255.00	7.66	[27]
<i>n</i> -tetradecane	279.00	45.07	71.22	194.00	0.18	[23], [27–28]
<i>n</i> -hexadecane	291.27	51.38	73.60	-	-	[23], [27], [29]–[31]
<i>n</i> -octadecane	301.26	61.08	71.43	-	-	[21], [23], [30]–[33]

^a Approximation from Ref. [21]

Table 2: Pure-component parameter for PC-SAFT non-associating substances

Compound	MW [g mol ⁻¹]	m^a [-]	σ^a [Å]	ϵ/k^a [K]	AAD% ^a	
					p^{sat}	v^j
<i>n</i> -hexane	86.1800	3.0576	3.7983	236.7700	0.3100	0.7600
<i>n</i> -undecane	156.3100	4.9082	3.8893	248.8200	2.0200	0.6900
<i>n</i> -tridecane	184.3600	5.6877	3.9143	249.7800	3.1500	1.7700
<i>n</i> -tetradecane	198.3900	5.9002	3.9396	254.2100	4.8000	1.2800
<i>n</i> -hexadecane	226.4400	6.6485	3.9552	254.7000	4.8800	0.7500
<i>n</i> -octadecane	254.4900	7.3271	3.9668	256.2000	4.9900	1.1900

^a Data from Ref. [15]

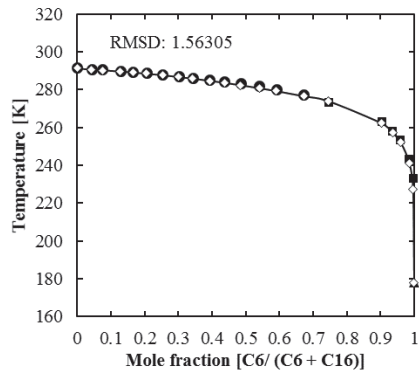


Figure 1: Wax disappearance temperature of *n*-hexane [C₆] + *n*-hexadecane [C₁₆] mixture at 1 bar. Comparison of PC-SAFT ($k_{ij} = 0$, —), and the regular solution theory (\diamond) to the experimental data. Reference: Exp. Data (\blacksquare) [36]. Exp. Data (\bullet) [37]. Exp. Data (\blacktriangle) [24].

The predicted VLE activity coefficients γ_i^L using PC-SAFT are the function of pure component parameters (m , σ , and ϵ/k), total densities (ρ), and binary interaction parameters (k_{ij}). Therefore, the precision of activity coefficients γ_i^L only depends on the accuracy of pure component parameters and the PC-SAFT performance. In this work, overall binary interaction parameters k_{ij} were set to zero based on the previous studies by Bender *et al.* [34] and Liang *et al.* [35]. Both studies

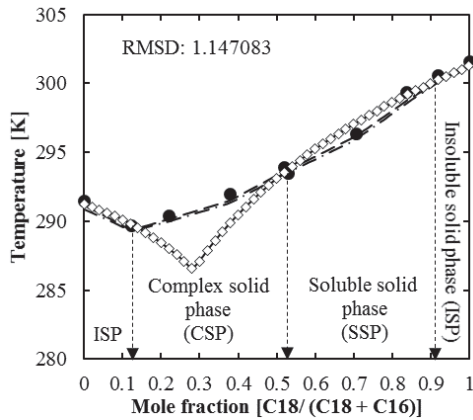


Figure 2: Wax disappearance temperature of *n*-octadecane [C₁₈] + *n*-hexadecane [C₁₆] mixture at 0.9 bar. Comparison of PC-SAFT ($k_{ij} = 0$, —), and the regular solution theory (◇) to the experimental data, Ideal liquid - predictive UNIQUAC solid (---) [3], and Ideal liquid - predictive Wilson solid (- · -) [3]. Reference: Exp. Data (●) [3].

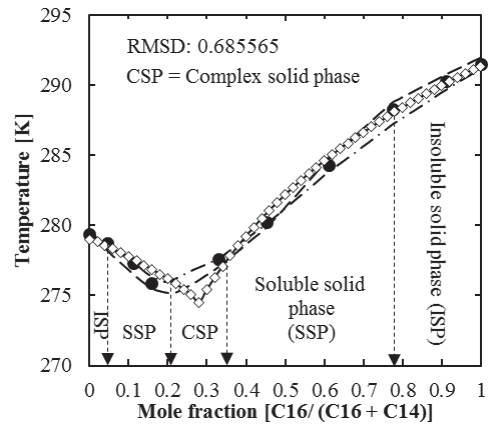


Figure 4: Wax disappearance temperature of *n*-hexadecane [C₁₆] + *n*-tetradecane [C₁₄] mixture at 0.9 bar. Comparison of PC-SAFT ($k_{ij} = 0$, —) with Equations (5) or (6), and the regular solution theory (◇) to the experimental data, Ideal liquid - predictive UNIQUAC solid (---) [3], and Ideal liquid - predictive Wilson solid (- · -) [3]. Reference: Exp. Data (●) [3].

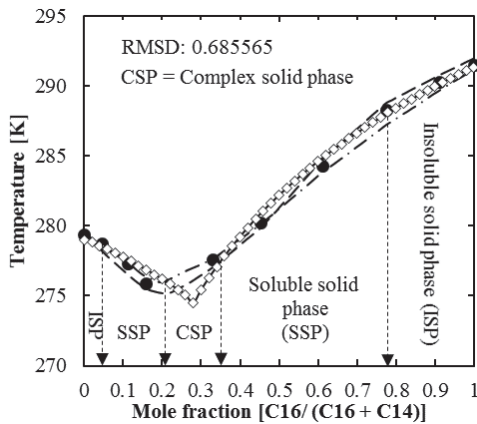


Figure 3: Wax disappearance temperature of *n*-hexadecane [C₁₆] + *n*-tetradecane [C₁₄] mixture at 0.9 bar. Comparison of PC-SAFT ($k_{ij} = 0$, —) with Equation (4), and the regular solution theory (◇) to the experimental data, Ideal liquid - predictive UNIQUAC solid (---) [3], and Ideal liquid - predictive Wilson solid (- · -) [3]. Reference: Exp. Data (●) [3].

showed the effect of the VLE estimation with k_{ij} of zero, ranging from 4–28 AAD% depending on the compound functional group. Furthermore, low AAD% found in the non-associating mixture, while

the associating mixture required values of k_{ij} for better results of VLE estimation. This means that the influence of k_{ij} can be minimized, especially for the *n*-alkane. Moreover, the optimization of the original PC-SAFT by Gross *et al.* [15] was based on the *n*-alkane as the chainlike-shape molecule. In addition, the k_{ij} interaction as described by Gross *et al.* [15] depended on the pair of compounds rather than the ratio of compositions. Consequently, the k_{ij} interaction between two *n*-alkane molecules is not required any adjustment, which is led to more simplified set-up for the estimation, especially in the multicomponent system.

The estimated results from PC-SAFT and the regular solution theory were compared as shown in Figures 1–4. The differences of the estimated WDT from both solutions were not significant. Therefore, the process of the estimation was acceptable to observe the influence of the provided solid assumption and phase-change properties to the accuracy of the estimated WDT.

It is worth mentioning that, both endpoints (at $x_i = 0$ and $x_i = 1$) of all estimated results are fixed to indicate temperature T at $T_{fus,i}$. The influence of the enthalpy of the crystalline transition term (ΔH_i^{fus} , $T_{fus,i}$, ΔH_i^{tr} , $T_{tr,i}$) to the estimated WDT of binary mixtures could be observed in Figures 1–6. Moreover, the heat capacity ΔC_p had already included in every estimated result.



Most of the results cannot observe the influence of this parameter due to the resolution on the present methodology, where more details were described later in the text.

Figures 1 and 2 represented the system of the crystalline I-liquid transition. The solutions indicated a close estimated trend, especially for the mixture of *n*-hexane + *n*-hexadecane [$C_6 + C_{16}$]. As shown in Figure 1, the melting point of pure *n*-hexane [C_6] and *n*-hexadecane [C_{16}] were 177.97 K and 291.27 K, respectively, which is 113.3 K difference. Practically, the component that has the highest melting temperature is considered to be the latest component to re-dissolve, which is *n*-hexadecane [C_{16}] in this case. For the thermodynamic perspective as referred to Equation (4), the latest component to re-dissolve is indicated by the component that is yielded the equality in this equation, which in this case is also *n*-hexadecane [C_{16}]. Moreover, due to the given solid assumption for a solid-phase, both *n*-hexadecane [C_{16}] and *n*-hexane [C_6] did not dissolve to each other, and it also showed the simple crystalline I-liquid transition.

Unlike the mixture of *n*-hexane + *n*-hexadecane [$C_6 + C_{16}$], the mixture of *n*-octadecane + *n*-hexadecane [$C_{18} + C_{16}$] showed the influence of the solid assumption with the deviation in the predicted results. As seen in Figure 2, the mole fraction of [$C_{18}/(C_{18} + C_{16})$] between 0.5–1, the predicted WDT were slightly higher than the experimental WDT. The adjustment of the solution by adding x_i^s and γ_i^s (as soluble solid-phase assumption) results in lowering the predicted WDT. For the mole fraction of [$C_{18}/(C_{18} + C_{16})$] ranging between 0.1–0.5 (eutectic area), the predicted results showed much lower WDT than the experimental results. This is possibly due to the fact that this region belongs to a complex solid-phase which requires the complex-solid solution.

The results of this work were different from Parsa *et al.* [3], which showed a perfect agreement by combining the ideal liquid model (VLE) with two different models for SLE: predictive Wilson (p.Wilson) and predictive UNIQUAC (p.UNIQUAC). The aims in Parsa *et al.*'s work is to find the capability and the best combination of different models. However, the assumption for SLE was not provided, where the model for SLE might be optimized to give the best fit results. This may not appropriately represent the phase behavior for both liquid-phase and solid-phase. Unlike this work which tried to give an appropriate solution for

VLE and the assumption for SLE, then the influence of each parameters and the provided assumption to the estimated WDT were considered.

Figure 5 shows the influence of the crystalline II-I transition of different pairs of mixtures, especially for the *n*-tridecane + *n*-hexane [$C_{13} + C_6$]. Even though, Equation (6) can provide the trend approach to the experiment, but the estimated result indicated the deviation at the mole fraction of [$C_{13}/(C_{13} + C_6)$] ranging between 0.5–1, which close to the pure state of *n*-tridecane [C_{13}]. Since the influence of the crystalline II-I transition term in Equations (5) and (6) tends to increase the overall temperature by increasing the enthalpy term (ΔH_i^{fus} , ΔH_i^{tr}). For the near pure state of *n*-tridecane [C_{13}], Equations (5) and (6) result in shifting the temperature down to the zone between the crystalline I-liquid transition to the crystalline II-I transition, due to two different transition temperatures ($T_{fus,i}$, $T_{tr,i}$).

Upon the observation, the provided solution is valid in a different scenario, where this can be represented in Figure 6. The SLE's description as in the form of Equations (5) and (6) is only valid whenever there is a contribution of the crystalline II-I phase transition. In contrast, Equation (4) is valid whenever there is only a contribution of the crystalline I-liquid phase transition. For the estimation of WDT, to select between two forms of SLE's description, there must be a function to identify the suitable condition for the individual mixture. Until this point, there was no clear description of this function, which the further study on this function should be conducted. In practice, Equation (4) is used whenever $T > T_{tr,i}$, and Equations (5) and (6) is used whenever $T < T_{tr,i}$. For the temperature T close to the transition temperature $T_{tr,i}$, all Equations (4)–(6) can be used.

Notice that in the *n*-tridecane + *n*-hexane [$C_{13} + C_6$] mixture, *n*-tridecane [C_{13}] has the melting temperature of approximately 80 K higher than the one of *n*-hexane [C_6]. Practically, this can indicate that the crystal of *n*-tridecane [C_{13}] would dissolve last due to the higher melting temperature. Generally, the crystal transition process is in sequential order as follows: crystalline III-II, crystalline II-I, and crystalline I-liquid, respectively. It should be pointed out that for a mixture of *n*-tridecane + *n*-hexane [$C_{13} + C_6$], the mole fraction of [$C_{13}/(C_{13} + C_6)$] ranging between 0–0.5, the crystalline transition was directly changed from crystalline III to liquid.

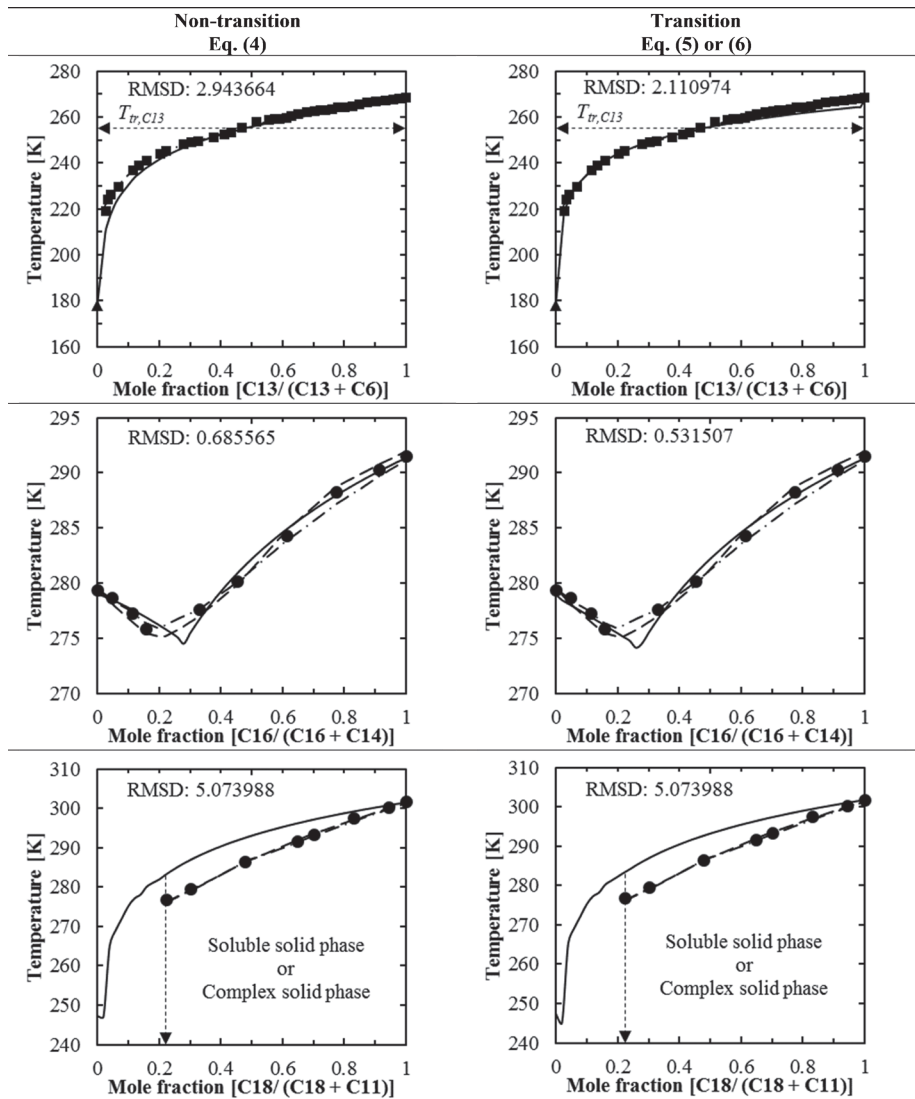


Figure 5: Wax disappearance temperature of binary mixture *n*-tridecane [C₁₃] + *n*-hexane [C₆] at 1 bar, *n*-hexadecane [C₁₆] + *n*-tetradecane [C₁₄] at 0.9 bar, and *n*-octadecane [C₁₈] + *n*-undecane [C₁₁] at 0.9 bar. Comparison of PC-SAFT ($k_{ij} = 0$, —) to the experimental data, empirical correlation (— · —) [38], Ideal liquid - predictive UNIQUAC solid (---) [3], and Ideal liquid - predictive Wilson solid (— —) [3]. Reference: Exp. Data (■) [38]. Exp. Data (▲) [24]. Exp. Data (●) [3].

Similar case of crystalline II-I transition, a mixture of *n*-hexadecane + *n*-tetradecane [C₁₆ + C₁₄], a deviation is observed when the mole fraction of [C₁₆ / (C₁₆ + C₁₄)] approaches to zero. Even though the difference between fusion temperature $T_{fus,i}$ and transition temperature $T_{tr,i}$ is significantly large, the deviation of WDT from the experimental values was not significant (only ±1 K).

This is possibly due to a small contribution of transition enthalpy ΔH_i^{tr} . It is worth noticing that the inclusion of transition in estimation leads to different results as obtained from Equation (5) (or Equation (6)) compared to that of Equation (4), as represented in

Figures 3 and 4 respectively. For the case of *n*-hexadecane + *n*-tetradecane [C₁₆ + C₁₄], Equation (4)

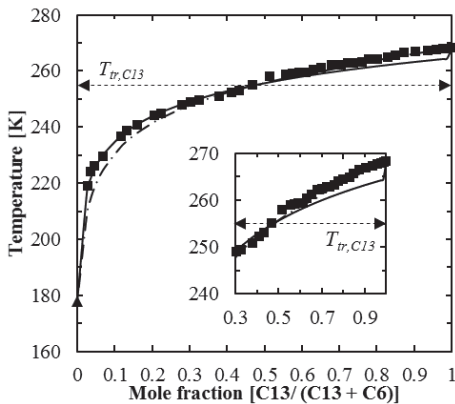


Figure 6: Wax disappearance temperature of *n*-tridecane [C_{13}] + *n*-hexane [C_6] mixture at 1 bar. PC-SAFT ($k_{ij} = 0$, —) with Equation (5) or (6), PC-SAFT ($k_{ij} = 0$, - - -) with Equation (4), Reference: Exp. Data (■) [38]. Exp. Data (▲) [24].

is more suitable because the transition temperature $T_{tr,i}$ is quite lower than the estimated WDT, leading to the soluble solid-phase region in the mole fraction of [$C_{16}/(C_{16} + C_{14})$] ranging between 0.05–0.2. While using Equation (5) (or Equation (6)) to a given system or pair lead to the shifting of the soluble solid-phase region in the mole fraction of [$C_{16}/(C_{16} + C_{14})$] ranging between 0.1–0.2. Since the experimental data were not fully provided, especially in the eutectic area, this may lead to slightly misled analysis.

For a mixture of *n*-octadecane + *n*-undecane [$C_{18} + C_{11}$] as shown in Figure 5, since the experimental data of *n*-octadecane + *n*-undecane [$C_{18} + C_{11}$] were not reported in the mole fraction of [$C_{18}/C_{18} + C_{11}$] ranging between 0–0.2, the behavior of solution is not perfectly observed for the whole range of mole fractions. Therefore, the hypothesis was made that the assumed value of WDT should follow estimated WDT obtained from the models. For this case, the difference of the melting temperature between *n*-octadecane [C_{18}] and *n*-undecane [C_{11}] is rather large, up to 50 K. For the trend of estimated results is quite similar to that of *n*-tridecane + *n*-hexane [$C_{13} + C_6$] case. However, large difference between experimental data and estimated value was observed due to the given solid assumption. The improvement of the model could be possibly done by applying both soluble solid assumption and complex solid assumption. Until this point, there was no clear description on the selection between these three solid-

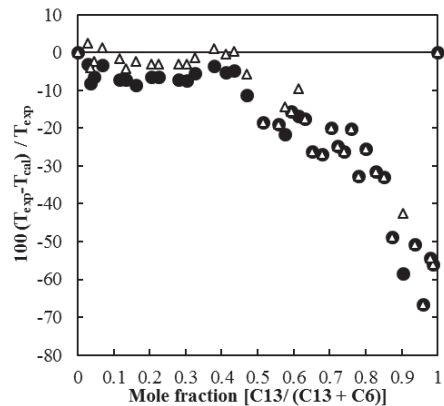


Figure 7: Error on the wax disappearance temperature of *n*-tridecane [C_{13}] + *n*-hexane [C_6] mixture at 1 bar. Comparison of the heat capacity influence to the prediction accuracy using Equation (5) or (6) with the crystalline II-I transition term: (●) Neglect the heat capacity contribution and (Δ) Include the heat capacity contribution.

phase assumptions. A possible solution is to find a function that can determine appropriate conditions for each of solid assumptions.

Most of mixtures could not observe the influence of the heat capacity $\Delta C_{p,i}$, except in the case of *n*-tridecane + *n*-hexane [$C_{13} + C_6$], as represented in Figure 7. The inclusion of the heat capacity to the estimation yielded slightly better accuracy on the estimated WDT.

The importance and the influence of each parameters for the estimation had been presented in this work. There are still improvements especially on the suitable description for solid-phase. However, this estimation with the use of only pure component parameter already have more beneficial for the industrial application.

5 Conclusions

In this work, the WDT for five different mixtures, including *n*-hexane + *n*-hexadecane, *n*-octadecane + *n*-hexadecane, *n*-tridecane + *n*-hexane, *n*-hexadecane + *n*-tetradecane, and *n*-octadecane + *n*-undecane were estimated using PC-SAFT EoS with multiple solid-phase model. The estimated result also confirmed by the regular solution theory. The provided the phase-change properties and the assumption were analyzed to find the influence on the estimated WDT, then the optimization could be suggested. Most of the estimated

WDT were in reasonable agreement with the experimental results, where the influence of the given parameters and the assumption could be described as follows:

1) In this present work, the enthalpy of the crystalline transition terms included the enthalpy of fusion ΔH_i^{fus} (as the crystalline I – liquid transition) and the enthalpy of transition ΔH_i^{tr} (as the crystalline II-I transition) were used to estimate the WDT. The good agreements with the experimental results were observed. Upon the observation, to logically estimate the WDT, the enthalpy of the crystalline transition terms (ΔH_i^{fus} and ΔH_i^{tr}) have to appropriately include in the solution, regarding to the phase on that condition.

2) For the WDT, the heat capacity $\Delta C p_i$ was assumed to be independent of temperature. The obtained result had shown a good improvement by including it, where this depended on its proportion comparing to the enthalpy term. This could be very essential for the estimation, especially in the multicomponent system.

3) In this work, the solid-phase assumption was divided into three zones according to the phase behavior, insoluble solid-phase, soluble solid-phase, and complex solid-phase. Based on the obtained result, the solid-phase assumption showed a significant impact on the accuracy of the estimation. Therefore, to properly select the suitable assumption for a particular mixture, it requires to know the mixture's behavior as well as the function.

Even though, this solution requires improvement, nevertheless, for the industrial application, it demonstrated many benefits from using only pure components to estimate the mixture property.

Acknowledgments

The authors would like to thank Bangchak Corporation Public Company for the financial support.

Nomenclature

f	Fugacity, Pa
x	Mole fraction
v	Molar volume, $\text{m}^3 \cdot \text{mol}^{-1}$
R	Gas constant, $\text{J} \cdot \text{mol}^{-1} \cdot \text{K}^{-1}$
T	Temperature, K
P	Pressure, Pa
ΔH	Enthalpy change, $\text{J} \cdot \text{mol}^{-1}$
ΔC	Heat capacity change, $\text{J} \cdot \text{mol}^{-1} \cdot \text{K}^{-1}$

A	Helmholtz free energy, J
N	Avogadro's number
k	Boltzmann constant, $\text{J} \cdot \text{K}^{-1}$
m	Compound's segment number
Z	Compressibility factor
MW	Molecular weight, $\text{g} \cdot \text{mol}^{-1}$
$D_{i,25}^L$	Liquid-phase density at 25°C defined by Equation (22), $\text{g} \cdot \text{cm}^{-3}$

Greek letters

γ	Activity coefficient
σ	Temperature-independent segment diameter, Å
ε	Segment dispersion energy parameter, J
φ	Fugacity coefficient
μ	Chemical potential, $\text{J} \cdot \text{mol}^{-1}$
η	Packing fraction
δ	Solubility parameters, $\text{MPa}^{1/2}$
$\bar{\delta}$	Mean solubility parameters, $\text{MPa}^{1/2}$
ϕ	Volume fractions

Sub and superscripts

L	Liquid
S	Solid
V	Vapor
p	Constant pressure
$pure$	Pure state of property
fus	Fusion state of property
tr	Transition state of property
res	Residual property
exp	Experimental property
cal	Calculated property

References

- [1] F. I. Mirante and J. A. Coutinho, "Cloud point prediction of fuels and fuel blends," *Fluid Phase Equilibria*, vol. 180, no. 1–2, pp. 247–255, 2001.
- [2] H. M. Meighani, C. Ghotbi, and T. J. Behbahani, "A modified thermodynamic modeling of wax precipitation in crude oil based on PC-SAFT model," *Fluid Phase Equilibria*, vol. 429, pp. 313–324, 2016.
- [3] S. Parsa, J. Javanmardi, S. Aftab, and K. Nasrifar, "Experimental measurements and thermodynamic modeling of wax disappearance temperature for the binary systems $n\text{-C}_{14}\text{H}_{30}^+$ $n\text{-C}_{16}\text{H}_{34}$, $n\text{-C}_{16}\text{H}_{34}^+$ $n\text{-C}_{18}\text{H}_{38}$ and $n\text{-C}_{11}\text{H}_{24}^+$ $n\text{-C}_{18}\text{H}_{38}$," *Fluid Phase*

- Equilibria*, vol. 388, pp. 93–99, 2015.
- [4] K. S. Pedersen, P. Skovborg, and H. P. Roenningsen, “Wax precipitation from North Sea crude oils. 4. Thermodynamic modeling,” *Energy & Fuels*, vol. 5, no. 6, pp. 924–932, 1991.
- [5] P. Leelavanichkul, M. D. Deo, and F. V. Hanson, “Crude oil characterization and regular solution approach to thermodynamic modeling of solid precipitation at low pressure,” *Petroleum Science and Technology*, vol. 22, no. 7–8, pp. 973–990, 2004.
- [6] H. Y. Ji, B. Tohidi, A. Danesh, and A. C. Todd, “Wax phase equilibria: Developing a thermodynamic model using a systematic approach,” *Fluid Phase Equilibria*, vol. 216, no. 2, pp. 201–217, 2004.
- [7] H. P. Roenningsen, B. Bjoerndal, A. B. Hansen, and W. B. Pedersen, “Wax precipitation from North Sea crude oils: 1. Crystallization and dissolution temperatures, and Newtonian and non-Newtonian flow properties,” *Energy & Fuels*, vol. 5, no. 6, pp. 895–908, 1991.
- [8] R. O. Dunn, “Crystallization behavior of fatty acid methyl esters,” *Journal of the American Oil Chemists’ Society*, vol. 85, no. 10, pp. 961–972, 2008.
- [9] F. Tumakaka, J. Gross, and G. Sadowski, “Thermodynamic modeling of complex systems using PC-SAFT,” *Fluid Phase Equilibria*, vol. 228–229, pp. 89–98, 2005.
- [10] A. Grenner, G. M. Kontogeorgis, N. von Solms, and M. L. Michelsen, “Modeling phase equilibria of alkanols with the simplified PC-SAFT equation of state and generalized pure compound parameters,” *Fluid Phase Equilibria*, vol. 258, no. 1, pp. 83–94, 2007.
- [11] M. Okuniewski, K. Padaszyński, and U. Domańska, “(Solid + liquid) equilibrium phase diagrams in binary mixtures containing terpenes: New experimental data and analysis of several modelling strategies with modified UNIFAC (Dortmund) and PC-SAFT equation of state,” *Fluid Phase Equilibria*, vol. 422, pp. 66–77, 2016.
- [12] F. Tumakaka, I. V. Prikhodko, and G. Sadowski, “Modeling of solid–liquid equilibria for systems with solid-complex phase formation,” *Fluid Phase Equilibria*, vol. 260, no. 1, pp. 98–104, 2007.
- [13] J. M. Prausnitz, R. N. Lichtenthaler, and E. G. de Azevedo, *Molecular Thermodynamics of Fluid-Phase Equilibria*. 3rd ed., New Jersey: Prentice Hall PTR, 1998.
- [14] M. Benziane, K. Khimeche, A. Dahmani, S. Nezar, and D. Trache, “Experimental determination and prediction of (solid + liquid) phase equilibria for binary mixtures of heavy alkanes and fatty acids methyl esters,” *Journal of Thermal Analysis and Calorimetry*, vol. 112, no. 1, pp. 229–235, 2013.
- [15] J. Gross and G. Sadowski, “Perturbed-chain saft: An equation of state based on a perturbation theory for chain molecules,” *Industrial & Engineering Chemistry Research*, vol. 40, no. 4, pp. 1244–1260, 2001.
- [16] K. W. Won, “Thermodynamics for solid solution-liquid-vapor equilibria: Wax phase formation from heavy hydrocarbon mixtures,” *Fluid Phase Equilibria*, vol. 30, pp. 265–279, 1986.
- [17] E. Stefanis and C. Panayiotou, “Prediction of hansen solubility parameters with a new group-contribution method,” *International Journal of Thermophysics*, vol. 29, no. 2, pp. 568–585, 2008.
- [18] K. S. Pedersen, “Prediction of cloud point temperatures and amount of wax precipitation,” *SPE Production & Facilities*, vol. 10, no. 1, pp. 46–49, 1995.
- [19] M. Wu and S. Yalkowsky, “Estimation of the molar heat capacity change on melting of organic compounds,” *Industrial & Engineering Chemistry Research*, vol. 48, no. 2, pp. 1063–1066, 2009.
- [20] G. D. Pappa, E. C. Voutsas, K. Magoulas, and D. P. Tassios, “Estimation of the differential molar heat capacities of organic compounds at their melting point,” *Industrial & Engineering Chemistry Research*, vol. 44, no. 10, pp. 3799–3806, 2005.
- [21] J. F. Messerly, G. B. Guthrie Jr., S. S. Todd, and H. L. Finke, “Low-temperature thermal data for pentane, *n*-heptadecane, and *n*-octadecane. Revised thermodynamic functions for the *n*-alkanes, C5-C18,” *Journal of Chemical and Engineering Data*, vol. 12, no. 3, pp. 338–346, 1967.
- [22] D. R. Douslin and H. M. Huffman, “Low-temperature thermal data on the five isomeric hexanes1,” *Journal of the American Chemical Society*, vol. 68, no. 9, pp. 1704–1708, 1946.
- [23] E. S. Domalski and E. D. Hearing, “Heat capacities

- and entropies of organic compounds in the condensed phase. volume III,” *Journal of Physical and Chemical Reference Data*, vol. 25, no. 1, pp. 1–525, 1996.
- [24] D. R. Stull, “A semi-micro calorimeter for measuring heat capacities at low temperatures1,” *Journal of the American Chemical Society*, vol. 59, no. 12, pp. 2726–2733, 1937.
- [25] H. M. Huffman, G. S. Parks, and M. Barmore, “Thermal data on organic compounds. X. further studies on the heat capacities, entropies and free energies of hydrocarbons,” *Journal of the American Chemical Society*, vol. 53, no. 10, pp. 3876–3888, 1931.
- [26] G. S. Parks, H. M. Huffman, and S. B. Thomas, “Thermal data on organic compounds. VI. the heat capacities, entropies and free energies of some saturated, non-benzenoid hydrocarbons1,” *Journal of the American Chemical Society*, vol. 52, no. 3, pp. 1032–1041, 1930.
- [27] H. L. Finke, M. E. Gross, G. Waddington, and H. M. Huffman, “Low-temperature thermal data for the nine normal paraffin hydrocarbons from octane to hexadecane,” *Journal of the American Chemical Society*, vol. 76, no. 2, pp. 333–341, 1954.
- [28] G. S. Parks and D. W. Light, “Thermal data on organic compounds. XIII. the heat capacities and entropies of *n*-tetradecane and the hydroxybenzoic acids. The relative free energies of some benzenoid position isomers,” *Journal of the American Chemical Society*, vol. 56, no. 7, pp. 1511–1513, 1934.
- [29] P. Claudy and J. M. Letoffe, “Phase transitions in even *n*-alkane C_nH_{2n+2} , $n=16-28$ Characterization by differential calorimetric analysis and by thermo-optical analysis. Effect of deuteration,” *Calorimetrie et Analyse Thermique*, vol. 22, pp. 281–290, 1991.
- [30] D. Mondieig, F. Rajabalee, V. Metivaud, H. A. J. Oonk, and M. A. Cuevas-Diarte, “*n*-alkane binary molecular alloys,” *Chemistry of Materials*, vol. 16, no. 5, pp. 786–798, 2004.
- [31] G. S. Parks, G. E. Moore, M. L. Renquist, B. F. Naylor, L. A. McClaine, P. S. Fujii, and J. A. Hatton, “Thermal data on organic compounds. XXV. Some heat capacity, entropy and free energy data for nine hydrocarbons of high molecular weight,” *Journal of the American Chemical Society*, vol. 71, no. 10, pp. 3386–3389, 1949.
- [32] P. Barbillon, L. Schuffenecker, J. Dellacherie, D. Balesdent, and M. Dirand, “Variation d'enthalpie subie de 260 K à 340 K par les *n*-paraffines, comprises entre l'octadécane ($n-C_{18}$) et l'hexacosane ($n-C_{26}$),” *Journal de Chimie Physique*, vol. 88, pp. 91–113, 1991.
- [33] S. I. Kolesnikov and Z. I. Syunyaev, “Phase transitions in the melting and crystallization of $n-C_{18}H_{38}$ and $n-C_{20}H_{42}$,” *Zhurnal Prikladnoi Khimii (Leningrad)*, vol. 58, no. 10, pp. 2267–2271, 1985.
- [34] N. Bender, N. S. M. Cardozo, and R. d. P. Soares, “Avoiding binary interaction parameters in the GC-PC-SAFT model with a parametrization based in VLE and IDAC data: *n*-Alkanes and 1-alkanols,” *Fluid Phase Equilibria*, vol. 412, pp. 9–20, 2016.
- [35] X. Liang, K. Thomsen, W. Yan, and G. M. Kontogeorgis, “Prediction of the vapor–liquid equilibria and speed of sound in binary systems of 1-alkanols and *n*-alkanes with the simplified PC-SAFT equation of state,” *Fluid Phase Equilibria*, vol. 360, pp. 222–232, 2013.
- [36] C. W. Hoerr and H. J. Harwood, “Solubilities of high molecular weight aliphatic compounds in *n*-hexane,” *The Journal of Organic Chemistry*, vol. 16, no. 5, pp. 779–791, 1951.
- [37] U. Domańska and K. Kniż, “Solid-Liquid Equilibria of Normal Alkanes (C_{16} , C_{18} , C_{20}) + Hexane, + 3-Methylpentane, + 2, 2-Dimethylbutane, or + Cyclohexane,” *Selected Data on Mixtures*, vol. 2, pp. 83–92, 1990.
- [38] P. Morawski, J. A. Coutinho, and U. Domańska, “High pressure (solid + liquid) equilibria of *n*-alkane mixtures: Experimental results, correlation and prediction,” *Fluid Phase Equilibria*, vol. 230, no. 1–2, pp. 72–80, 2005.